Transport Layer Delay Analysis in Wireless Networks using Signal Flow Graphs

Guido Gehlen, Bernhard Walke
RWTH Aachen University, Faculty 6
Communication Networks
Kopernikusstr. 16, 52074 Aachen
guge@comnets.rwth-aachen.de

***Abstract*— The performance of transport layer protocols in wireless networks is difficult to analyze due to the behavior of the underlying wireless link layer. This paper presents a novel analytical modeling method for transport layer error control mechanisms in wireless networks. The layered modeling method presented is based on packet delay distributions which are derived from a link layer model regarding correlated radio block errors and a link layer Selective Repeat ARQ (SR-ARQ) mechanism. A canonical Hidden Markov Model (HMM) is used to model correlated radio block errors. The SR-ARQ on link layer, that corrects these block errors, is modeled by means of a matrix signal flow graph representing statistically the delays caused by correlated block errors. The modeling method on transport layer uses extended signal flow graphs where edges are weighted by Moment Generating Functions (MGFs) of the packet transmission delay. Results are presented in terms of applying the modeling method to a simple ARQ on top of UDP. The link layer model used is parameterized for GPRS.**

I. Introduction

Transport layer delay analysis have to take the variances of network layer packet transmissions into account, especially by comprising wireless links. State-of-the-art statistical Automatic Repeat Request (ARQ) analysis, as presented in [1] and [2] are no longer applicable, since they are based on a fixed packet transmission delay. This paper presents a transport layer ARQ model based on the approaches of [1], [2], and [3] extended by a method of considering packet delay variations.

The overall analytical model is based on a channel modeled by a canonical HMM. This model generates correlated radio block errors which are used to derive radio block transmission delay statistics on link layer by means of a matrix Signal Flow Graph (SFG) ARQ model. The resultant statistics in terms of delay distributions are the basis to derive transmission delays on Internet Protocol (IP) layer. The transmission delay on transport layer can be derived using the model presented in the following. The method is universally valid for all kind of transport layer protocols. Exemplarily, a SR-ARQ mechanism with explicit requests and cumulative NACKs on top of User Datagram Protocol (UDP) is modeled. The ARQ has a fixed windows size and is in particular useful for transmission of short-lived data flows.

II. Wireless Channel Model and Physical Layer Model

Wireless channels are characterized by a non-stationary behavior and signal distortions due to fading, interferences, shadowing, noise, and non-linearities. Hence, the error rate is high and not constant over time. Channel errors arise in bursts and are, thus, highly correlated.

The applied analytical model uses the Block Error Ratio (BLER) as starting point to model the wireless channel and physical layer. In order to model wireless channels with memory, i.e. the BLER is changing during the transmission and the values are correlated, a HMM is used. HMMs have been proved theoretically and experimentally [4] to be qualified for that purpose.

The average block transmission delay D_{Block} is dependent on physical layer properties, like the Modulation and Coding Scheme (MCS). Basically, D_{Block} is associated to the bandwidth r and the number of bit per radio block n_{Block}

$$D_{Block} = n_{Block}/r \tag{1}$$

This fixed block transmission delay is used to quantize the timeline into discrete values $t_k = k \cdot \Delta T$, with $\Delta T = D_{Block}$ and $k \in \mathbf{N}$. The time axis is, therefore, slotted and during each timeslot n_{Block} bits are transmitted. Such systems are called discrete-time systems (DTS) [1].

Generally, the block error rate behavior can be modeled by using a HMM with L finite channel states. Each state hides the block error rates with value ϵ_i $(i = 1 \ldots L)$. The transitions between the channel states are statistically described by transition probabilities p_{ij} from state i to state j. As a whole, all transition probabilities are collected in the channel transition matrix $\mathbf{P}$, where i is the row index and j the column index.

The hidden block error rates (BLER) are consolidated in the row vector

$$\boldsymbol{\epsilon} = (\epsilon_1, ..., \epsilon_L)\,, \quad 0 < \epsilon_i \leq 1 \quad \forall i \tag{2}$$

The most common used channel model is the canonical 2-state HMM, also known as Gilbert-Elliott model [5], [6], with a “Good” (state index 1) and “Bad” (state index 2) channel state. Each state hides the BLERs $\epsilon_1 = 0$ and $\epsilon_2 = 1$.

The channel state transition probability matrix of the 2-state HMM can be further reduced, since the sum of all outgoing probabilities per channel state is equal to 1.

$$\mathbf{P} = \begin{pmatrix} p_{11} & p_{12} \\ p_{21} & p_{22} \end{pmatrix} = \begin{pmatrix} 1-p_{12} & p_{12} \\ p_{21} & 1-p_{21} \end{pmatrix} \quad (3)$$

In general a HMM channel model is characterized by the state transition matrix $\mathbf{P}$, the error probability vector $\boldsymbol{\epsilon}$ and the initial probability state vector $\boldsymbol{\pi_0}$. After shifting the channel states k-times, the channel state probability is

$$\boldsymbol{\pi}_k = \boldsymbol{\pi}_0 \cdot \mathbf{P}^k \quad (4)$$

The stationary vector π of the HMM is the equilibrium probability vector of the channel states and can be derived through

$$\boldsymbol{\pi} \cdot \mathbf{P} = \boldsymbol{\pi} \quad (5)$$
$$\boldsymbol{\pi} \cdot \mathbf{1} = \mathbf{1} \quad (6)$$

The stationary vector of the two-state HMM is

$$\boldsymbol{\pi} = \left(\frac{p_{21}}{p_{12}+p_{21}}, \frac{p_{12}}{p_{12}+p_{21}} \right) \quad (7)$$

The average block error rate is

$$\overline{BLER} = \boldsymbol{\pi} \cdot \boldsymbol{\epsilon}^T = \frac{p_{12}}{p_{12}+p_{21}} \quad (8)$$

The channel transition probabilities viewed jointly with the channel observation Ch_k at a time k ($X(k) = 1$ for a radio block error, $X(k) = 0$ for an error-free transmission) are

$$\begin{aligned} prob(Ch_k = j, X(k) = 1 \,|\, Ch_{k-1} = i) &= p_{ij} \cdot \epsilon_j \\ prob(Ch_k = j, X(k) = 0 \,|\, Ch_{k-1} = i) &= p_{ij} \cdot (1-\epsilon_j) \end{aligned} \quad (9)$$

Collecting these probabilities into the conditional probability matrices $\mathbf{P_1}$ and $\mathbf{P_0}$ it follows for the canonical 2-state HMM

$$\mathbf{P_1} = \mathbf{P} \cdot diag\{\boldsymbol{\epsilon}\} = \begin{pmatrix} 0 & p_{12} \\ 0 & 1-p_{21} \end{pmatrix} \quad (10)$$
$$\mathbf{P_0} = \mathbf{P} \cdot diag\{\mathbf{1}-\boldsymbol{\epsilon}\} = \begin{pmatrix} 1-p_{12} & 0 \\ p_{21} & 0 \end{pmatrix} \quad (11)$$

The following relationship exists

$$\mathbf{P_0} + \mathbf{P_1} = \mathbf{P} \quad (12)$$

The outcome of the model is a discrete time random process $X(k)$ which indicates an block error ($X(k) = 1$) or a correct block transmission ($X(k) = 0$). Thus, the probabilities p_1 and p_2 of the states are

$$\begin{aligned} p_1 &= 1 - \overline{BLER} \\ p_2 &= \overline{BLER} \end{aligned} \quad (13)$$

The probability state transition probability p_{22} is equal to the conditional probability of two consecutive block errors

$$p_{22} = prob(X(k) = 1|X(k-1) = 1) \quad (14)$$

III. Mobile Link Layer Model

The channel state transition matrix $\mathbf{P}$ and the BLERs $\boldsymbol{\epsilon}$ of the channel model are used in the mobile link layer model jointly to compute the delay distribution of successful radio block transmissions. For calculations concerning the link layer ARQ, the notation and analysis of [1] and [3] are applied, where matrix probabilities and matrix signal flow graphs are used to analyze throughput and delay of ARQ mechanisms.

In most of the mobile communication systems a SR-ARQ protocol is used, since it is more efficient in terms of throughput compared to Stop-and-Wait and Go-Back-N protocols. The reason for the bandwidth efficiency is that only lost frames are retransmitted, subsequent frames, which are correctly received, are stored in the buffer. The disadvantage of the SR-ARQ is, therefore, that a larger buffer size is needed.

Analysis of ARQ protocols are accomplished amongst others by the research groups Lu, Chang [7], [2] and Turin, Zorzi, Badia, Rossi [1], [8]. The presented analysis orients on these analyses. The ARQ model of the link layer is slightly simple, but due to the separation of the analytical models, a more complex model can be applied without loss of generality.

Here, the ARQ is modeled by means of a SFG analysis, first used by Mason in [9]. The statistical states are the nodes and the transitions between them are weighted with a transition probability and a coefficient. In the case of a delay analysis, the delay operator z is used as weight coefficient, which was first proposed in [7].

In [7] and [2] scalar transition probabilities are used. However, this model is only applicable for non-correlated channels with one constant BLER. Taking the channel error correlations from Section II into account, the weight coefficients of the SFG are matrices. The resulting graph is called matrix Signal Flow Graph (SFG) [1], [3]. The matrix SFG of the SR-ARQ is depicted in Figure 1.

As mentioned before, the transmission delay of one radio block has a constant value of D_{Block}. This time is used to clock the time in the HMM channel model. Each D_{Block}-times the channel transits to another state according to the state transition probability matrix $\mathbf{P}$ and, supplementary, the ARQ model transits to the next node. The delay operator z correspond to the delay time D_{Block}.

The matrix signal flow graph of transmitting successfully one radio block by using the described SR-ARQ protocol over an erroneous forward HMM channel is depicted in Figure 1.

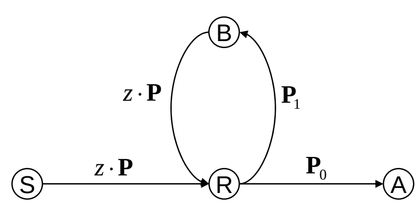

Fig. 1. Matrix signal flow graph of SR ARQ with error-free feedback channel

Starting from the Sending state (S) where the radio block is transmitted, the following state (R) is definitely reached after a delay of D_{Block}, indicated by the delay operator z. While moving to this state also the channel state of the HMM changes. Thus, the link from (S) to (R) is in addition weighted with the channel state transition probability matrix $\mathbf{P}$. In state (R) the receiver checks whether a radio block is acknowledged or not. If the block is acknowledged, the transmission is finished and the state (A) is reached with the probability $prob(Ch_k = j, X(k) = 0|Ch_{k-1} = i) = p_{ij} \cdot (1 - \epsilon_j)$. Thus, this link is weighted with the probability matrix $\mathbf{P_0}$. In case that a non-acknowledgement has been received, the state (B) is reached with the probability matrix $\mathbf{P_1}$, see Eq. (10). After the retransmission (SFG transition from (B) to (R) with $z\,\mathbf{P}$) the receiver checks again for the acknowledgement.

The overall matrix Moment Generating Function (MGF) $\mathbf{G_{SR}}(z)$ is derived by applying basic signal flow graph reduction rules [9]. The matrix $\mathbf{I}$ is the $L \times L$ unit matrix.

$$\mathbf{G_{SR}}(z) = z\,\mathbf{P}(\mathbf{I} - z\,\mathbf{P_1}\,\mathbf{P})^{-1}\mathbf{P_0} \tag{15}$$

The scalar moment generating function $G_{SR}(z)$ is obtained from the corresponding matrix moment generating function by pre-multiplying with the probability vector of transmitting a new block $\boldsymbol{\pi}_I$ and post-multiplying with the column vector of ones $(\mathbf{1})$ [1].

$$G_{SR}(z) = \frac{\boldsymbol{\pi}_I\,\mathbf{G_{SR}}(z)\,\mathbf{1}}{\boldsymbol{\pi}_I\,\mathbf{1}} \tag{16}$$

with

$$\boldsymbol{\pi}_I = \boldsymbol{\pi} \cdot \mathbf{P_0} \tag{17}$$

The delay distribution, i.e. the probability mass function of the delay P_{SR}, is derived either from the k-times differentiation or from the inverse z-transformation.

$$P_{SR}(k) = \frac{1}{k!} \cdot \left(\frac{\partial^k}{\partial z^k} G_{SR}(z) \right)_{z=0} = Z^{-1}(G_{SR}(z^{-1})) \tag{18}$$

In this case, the probability mass function of the delay can easily be computed. Calculating, first, the matrix MGF by inserting the following matrices in Eq. (15)

$$\mathbf{P_1} = \begin{pmatrix} 0 & p_{12} \\ 0 & 1 - p_{21} \end{pmatrix} \tag{19}$$

$$\mathbf{P_0} = \begin{pmatrix} 1 - p_{12} & 0 \\ p_{21} & 0 \end{pmatrix} \tag{20}$$

Applying Eq. (16), the resultant scalar MGF is

$$G_{SR}(z) = z \cdot \frac{(p_{21} + p_{12} - 1) \cdot z + 1 - p_{12}}{(p_{21} - 1) \cdot z + 1} \tag{21}$$

The corresponding probability mass function is derived to

$$\begin{aligned} P_{SR}(k) =& (p_{12} + p_{21} - 1) \cdot \Theta(k-2) \cdot (1 - p_{21})^{(k-2)} \\ & + (1 - p_{12}) \cdot \Theta(k-1) \cdot (1 - p_{21})^{(k-1)} \end{aligned} \tag{22}$$

$\Theta(k)$ is the discrete Heaviside or unit step function. Figure 2 depicts the probability mass function of the radio block delay after SR-ARQ for different average BLERs (p_2) and conditional error probabilities (p_{22}). Some parameter combinations of p_2 and p_{22} are not possible, since otherwise the conditional probability p_{12} would be greater than 1 ($p_{22} \geq 2 - 1/p_{22}$).

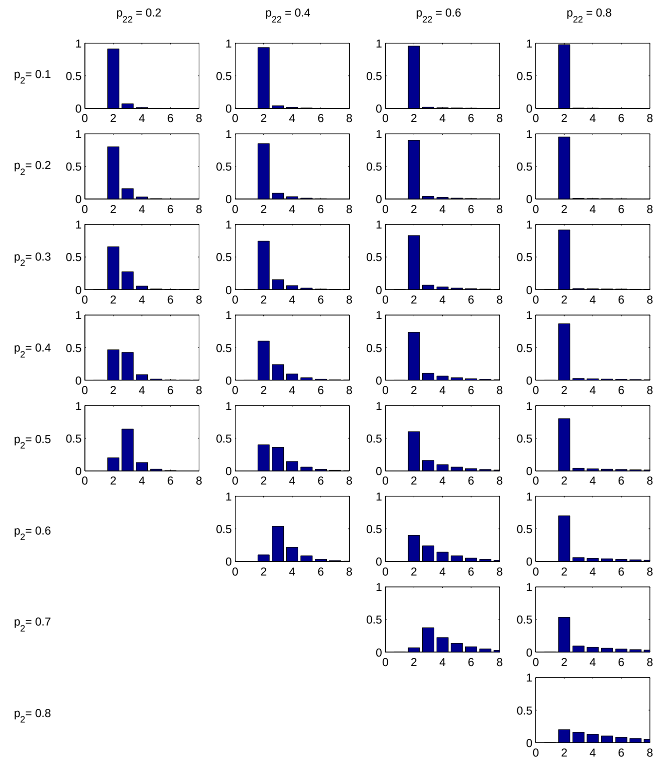

Fig. 2. Delay Distribution SR ARQ over 2-state Markov Model ($p_{22} \geq 2 - 1/p_{22}$)

The Figure shows that a higher correlation between subsequent block errors lead to a higher probability of the delay $k = 1$, but also to a higher variance due to the increase of the error burst length. If the channel is in the error state "2", the probability is higher to stay there. The SR-ARQ reacts with multiple retransmissions.

IV. Delay Distribution on IP Layer

Assuming an IP packet is fragmented into N radio blocks. The delay of an IP packet over a wireless link is, therefore, the sum of all related radio block delays. The correspondend MGF of the IP packet delay can be derived to

$$G_{IP}(z) = \frac{\boldsymbol{\pi}_I\,(\mathbf{G_{SR}}(z))^N\,\mathbf{1}}{\boldsymbol{\pi}_I\,\mathbf{1}} = (G_{SR}(z))^N \tag{23}$$

even if the correlation of subsequent radio blocks is regarded. The result is equal to the case that the delay of subsequent radio blocks is statistically independent. This is not generally the case, but applies for the idealized SR-ARQ algorithm.

Figure 3 shows the delay of transmitting IP packets of size 1024 byte in uplink and downlink direction for a General Packet Radio Service (GPRS) system using Coding Scheme CS-2. The channel correlation is set to $p_{22} = 0.8$ and p_2 varies from 0.1 to 0.4.

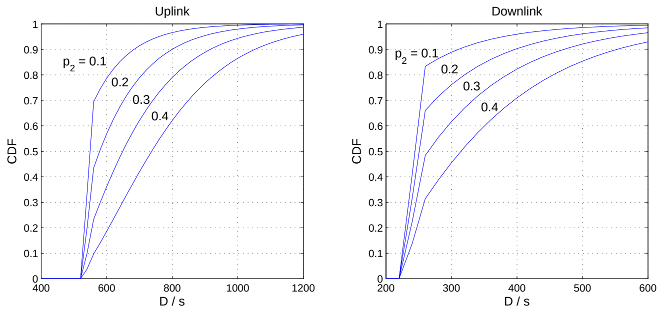

Fig. 3. Delay CDF of transmitting an IP packet of 1024 byte over GPRS with CS-2 in uplink (left) and downlink (right) direction, canonical HMM channel with $p_{22} = 0.8$, $p_2 = 0.1 \ldots 0.4$

V. Delay Analysis of Transport Layer ARQ

In order to comprise the IP delay statistics on transport layer, the SFG analysis model has to be extended. The link layer ARQ model described in the last section and in [2], [3] uses a deterministic delay (z) from one node of the SFG to another.

On transport layer the IP packets are delayed by a value of D_{IP} with an arbitrary probability mass function $P_{IP}(k)$. The delay is modeled as a discrete random process of values $k \in \mathbf{N}$. The moment generating function of D_{IP} is respectively $G_{IP}(z)$.

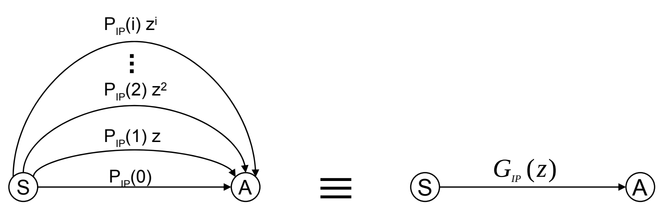

Fig. 4. Signal Flow Graph of a delayed segment transmission

Figure 4 illustrates a transmission of a segment over an error free channel with the varying delay D_{IP} using a SFG with the nodes "Sending" (S) and "Arrival" (A). The transmission from (S) to (A) is delayed by $k = 0$ units with the probability $P_{IP}(0)$, by $k = 1$ units with probability $P_{IP}(1)$ and so on. Thus, the whole transmission process, from (S) to (A), can be statistically described by the generating function $G_{IP}(z) = P_{IP}(0) + P_{IP}(1) \cdot z + \ldots$ as illustrated in Figure 4.

Transport layer protocols are modeled by means of assembling a SFG from the possible protocol states and assigning transition probabilities and delay MGFs to the state transitions. Protocol timeouts can be included in the model by weighting a transition with z^T, where T is the timeout value.

The resulting MGF of the transport layer delay $G_{tr}(z)$ can be transformed either analytically to the probability mass function, or the specifying equation of $G_{tr}(z)$ can be transformed in sections and derived numerically in the co-domain by using convolutional operations.

$$P_{tr}(k) \quad \circ\!\!-\!\!\bullet \quad G_{tr}(z^{-1}) \tag{24}$$

VI. Delay Analysis of SR-ARQ over UDP

In order to illustrate the capability of the model, a Selective-Repeat explicit request ARQ mechanism with cumulative bitmap based NACKs is modeled. The states of the sender and receiver are depicted in Figure 5. First, a bulk of n segments are sequentially transmitted. If no segments get lost, the receiver sends an ACK which results in finishing the transmission process. If one or more segments get lost, the receiver sends a NACK with a bitmap indicating the sequence numbers of the lost segments. These segments are retransmitted and again the receiver checks if any segment is missing. This procedure is repeated until all segments reach the receiver.

A. SR ARQ Analysis without ACK/NACK errors

The SFG representation of the SR-ARQ delay behavior without ACK/NACK errors is depicted in Figure 6. The delay of sending n segments is equal to the transition from the state (S) to (A) with the MGF $G_n(z)$. The MGF can be recursively deduced, since after sending n segments (transition form (S) to (R_0)), $i \leq n$ faulty segments have to be retransmitted (transition from (R_0) via (R_i) to (A)).

The probability that i of n segments are erroneous is $p_n(i)$. The retransmission starts not until the NACK has been received, therefore the transition from (R_0) to (R_i) is delayed by the $D_{NACK} = D_{ACK}$ with the MGF $G_{NACK}(z) = G_{ACK}(z)$.

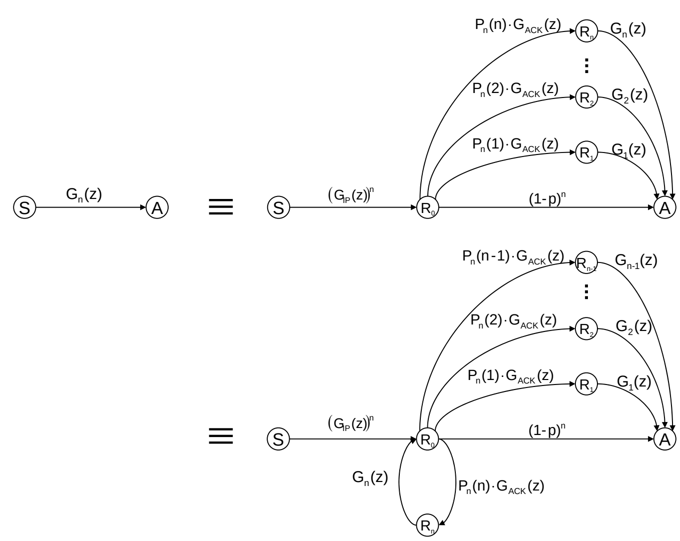

Fig. 6. Signal Flow Graph of the SR ARQ disregarding feedback errors and timeouts

After evaluating the NACK bitmap, i segments are retransmitted with the same procedure, thus, the retransmissions (transitions from (R_i) to (A)) are recursively delayed by $G_i(z)$. The recursive equation of the resulting MGF is

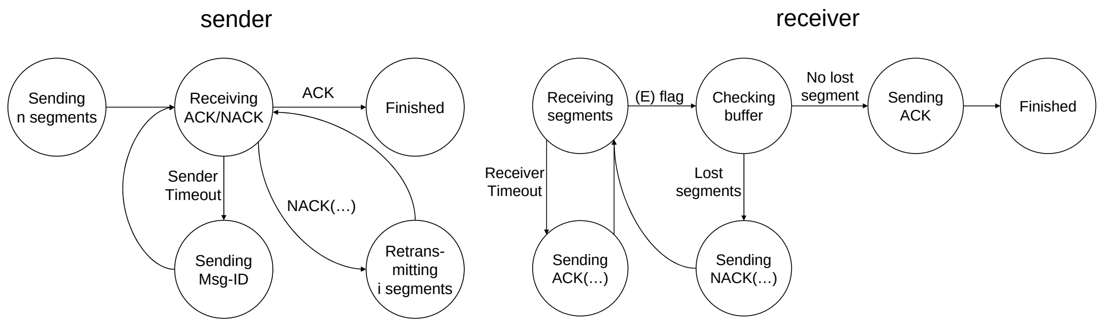

Fig. 5. States and transitions of the Selective-Repeat ARQ protocol

$$
\begin{aligned}
G_n(z) &= (G_{IP}(z))^n \left((1-p)^n + \sum_{i=1}^{n} p_n(i) G_{ACK}(z) G_i(z) \right) \\
&= G_F(z) \left((1-p)^n + G_{ACK}(z) \sum_{i=1}^{n-1} p_n(i) G_i(z) \right) \\
G_F(z) &= \frac{(G_{IP}(z))^n}{1 - p^n\, G_{ACK}(z)\, (G_{IP}(z))^n} \\
p_n(i) &= \binom{n}{i} \cdot p^i \cdot (1-p)^{(n-i)}
\end{aligned} \tag{25}
$$

The last element of the sum ($i = n$) from Eq. (25) can be extracted. The result is represented in the lower SFG of Figure 6 where the summand $p_n(n)\, G_{ACK}(z)\, G_n(z)$ is moved to the self-loop from (R_0) via (R_n) to (R_0). Generally, the recursion cannot be transformed into a non-recursive representation. In the following, the Eq. (25) is discussed by making some assumptions.

Assuming that a segment is transmitted with a deterministic delay of $D = 1$ unit, the corresponding MGF is $G_{IP}(z) = z$, and disregarding the acknowledgement delay ($G_{ACK}(z) = 1$) the recursion can be resolved to

$$G_n(z) = \frac{(1-p)^n\, (G_{IP}(z))^n}{1 - p\, (G_{IP}(z))^n} \tag{26}$$

This function is equal to a SR-ARQ where each segment is acknowledged. The average delay is the first derivative of the moment generating function at $z = 1$.

$$\overline{D}_n = G_n^{(1)}(1) = \frac{n}{1-p} \tag{27}$$

Thus, the total mean delay of transmitting m segments is respectively

$$\overline{D}_m = r \cdot \overline{D}_n = \frac{m}{1-p} \tag{28}$$

B. SR-ARQ Analysis in Consideration of ACK/NACK Errors

If the feedback channel is unreliable (ACKs and NACKs are disturbed as well), the timeouts of the ARQ protocol have to be included into the analysis. If both timers, sender and receiver timers are considered, the delay analysis is substantially more complex.

After analyzing the behavior of the sender and receiver timers in various conditions, it can be concluded that the receiver timers can be disregarded in the delay calculation, since the sender timer expires in advance. Assuming that the sender timeouts after exceeding the time T with a probability of p_T, the sender notifies the receiver by sending a timeout message. This message triggers the receiver to recheck the receive buffer and to answer with an ACK or NACK.

The corresponding SFG shown in Figure 7 can be deduced from Figure 6 by inserting a timeout state (T). The timeout state enters with a probability of p_T and induces a delay of T. After the timeout expires the sender stays in the timeout state with the probability p_T or transits with the probability $(1-p_T)$ and an additional delay of D_{MID} into the state (R_0). The further transitions from (R_0) to (A) remain unchanged to the case without any feedback errors.

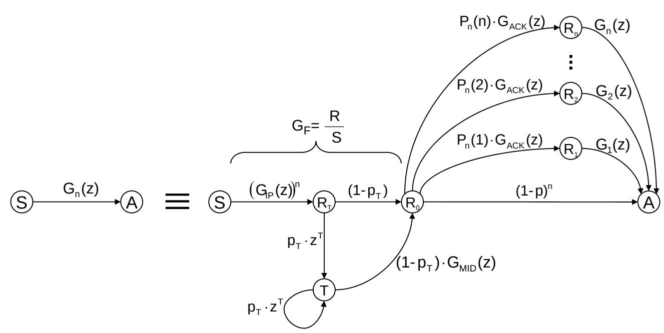

Fig. 7. Signal Flow Graph of the SR ARQ regarding feedback errors and sender tmeouts

From the SFG of Figure 7 the MGF of the transmission delay can be derived with the recursion

The timeout probability p_T is composed of the probabilities that the last segment gets lost or that an ACK or NACK segment gets lost (p_{ACK}) under the condition that the last segment has been received. Additionally, a segment loss occurs if the segment round-trip time (RTT) exceeds the timeout time.

$$p_T = p_{SL} + (1-p)\ (p_{ACK} + prob(RTT > T)) \approx p_{SL} \tag{30}$$

$$
\begin{aligned}
G_n(z) =& G_F(z) \cdot \left((1-p)^n + \sum_{i=1}^{n-1} P_n(i) \cdot G_{ACK}(z) \cdot G_i(z) \right) \\
G_F(z) =& \frac{(1-p_T)\,(G_{IP}(z))^n\,\left[1 + p_T\, z^T\,(1 - G_{MID}(z))\right]}{1 - p_T\, z^T\, - (1-p_T)\,p^n\,(G_{IP}(z))^n\, G_{ACK}(z)\,\left[1 + p_T\, z^T\,(1 - G_{MID}(z))\right]} = \frac{G_H(z)}{1 - p_T\, z^T - p^n\, G_{ACK}(z)\, G_H(z)}
\end{aligned} \tag{29}
$$

In the following the timeout probability p_T is approximated by the segment loss probability p_{SL} since $prob(RTT > T)$ and p_{ACK} can be assumed to be small.

In order to derive the delay statistics on transport layer, the delay of the SR-ARQ on top of UDP referred by $G_n(z)$ has to be iteratively solved from Eq. (31) either in the z-domain or in the co-domain. To avoid intensive derivations of inverse z-Transforms or (k)-times differentiation, the recursion is derived in the co-domain. Consequently, the multiplications, divisions are transformed to convolution $(*)$ and de-convolution $(*^{-1})$ operations.

The Eq. (31) is evaluated for a GPRS transmission (CS-2, multislotclass 10) using the canonical HMM channel model for $p_2 = 0.1$ and $p_{22} = 0.8$. Figures 8, 9, 10, 11, 12, and 13 show the results for a 1, 5, or 10 kbyte data transmission separated into up- and downlink transmission. Each figure depicts on the left the Probability Mass Function (PMF) and on the right side the integrated Cumulative Distribution Function function for different segment loss probabilities $p_{SL} = p$. The influence of segment losses is, in particular, cognizable in the delay distributions (left plots). In case of a 1024 byte transmission (Figure 8) only one datagram is sent with following retransmissions. The first retransmission is finished approximately 400 ms (uplink) or 250 ms (downlink) after the regular transmission.

In the case of transmitting 5 kbyte or 10 kbyte messages, various retransmission combinations occur and the probability of a retransmission based on one message increases. Furthermore, the probability of multiple retransmissions grows.

A prototype implementation of the protocol is used in [10] to transmit Simple Object Access Protocol (SOAP) messages in Mobile Web Service applications. The presented measurement results of average delay values comply to the analytical results presented.

VII. Conclusion and Outlook

The paper has presented a novel method of calculating the delay probability mass function of ARQ protocols on transport layer using signal flow graph analysis. The model takes the discrete transmission delay distribution of IP packets and packet losses into account. The analysis has been validated by modeling a SR-ARQ with explicit requests and bitmap based cumulative NACKs.

This analytical model differs from related models due to the fact that ACK/NACK errors are no longer disregarded and that the delay of one segment transmission can be arbitrarily distributed. Further analysis comprise a model of TCP in order to compare the behavior of different ARQ mechanisms on transport layer with TCP. Especially, the analysis of short-lived data flows, like Remote Procedure Calls (RPCs), over a wireless channel are considered.

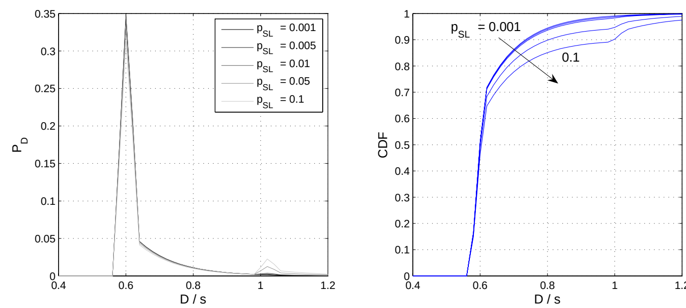

Fig. 8. SR-UDP delay of transmitting 1 kbyte, GPRS uplink, CS-2, MM $p_{22} = 0.8, p_2 = 0.1$ regarding segment losses of $p_{SL} = p$

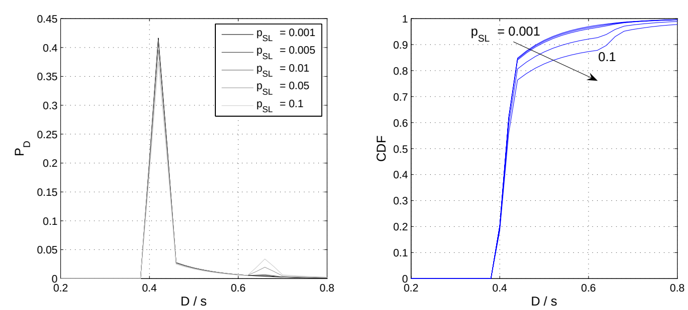

Fig. 9. SR-UDP delay of transmitting 1 kbyte, GPRS downlink, CS-2, MM $p_{22} = 0.8, p_2 = 0.1$ regarding segment losses of $p_{SL} = p$

References

[1] W. Turin, *Performance Analysis and Modeling of Digital Transmission Systems*, 3rd ed., W. Turin, Ed. Kluwer Academic, May 2004.

[2] D.-L. Lu and J.-F. Chang, "Performance of ARQ Protocols in Nonindependent Channel Errors," *IEEE Transactions on Communications*, vol. 41, no. 5, p. 721, Mar 1993. [Online]. Available: http://ieeexplore.ieee.org/xpl/freeabs_all.jsp?tp=&arnumber=225487

[3] K. Ausavapattanakun and A. Nosratinia, "Analysis of selective repeat arq via matrix signal flow graphs," *IEEE Transactions on Wireless Communications*, jun 2005.

[4] W. Turin, R. Jana, C. Martin, and J. Winters, "Modeling wireless channel fading," in *Vehicular Technology Conference, 2001. VTC 2001 Fall. IEEE VTS 54th*, vol. 3, 7-11 Oct. 2001, pp. 1740–1744vol.3.

[5] E. Gilbert, "Capacity of a burst-noise channel," *Bell Syst. Tech. J*, vol. 39, no. 5, pp. 1253–1265, 1960.

[6] E. Elliott, "Estimates of error rates for codes on burst-noise channels," *Bell Syst. Tech. J*, vol. 42, no. 9, pp. 1977–1997, sept 1963.

$$
\begin{aligned}
P_n(k) &= P_F(k) * \left((1-p)^n\, \delta(k) + \sum_{i=1}^{n-1} P_n(i) \cdot P_{ACK}(k) * P_i(k) \right) \\
P_F(k) &= P_H(k) *^{-1} \left[\delta(k) - p_T\, \delta(k-T) - p_n\, P_{ACK}(k) * P_H(k) \right] \\
P_H(k) &= (1-p_T)\,(P_D(k))^{*n} * \left[\delta(k) + p_T\, (\delta(k-T) - P_{MID}(k-T)) \right]
\end{aligned} \tag{31}
$$

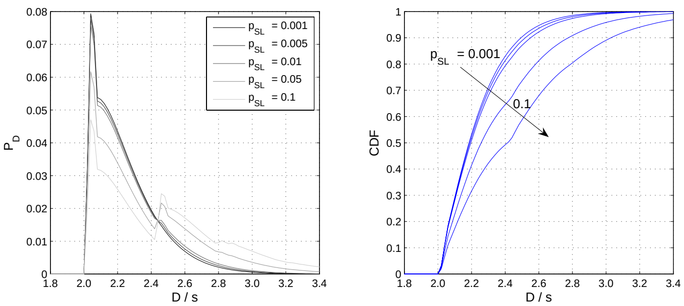

Fig. 10. SR-UDP delay of transmitting 5 kbyte, GPRS uplink, CS-2, MM $p_{22} = 0.8, p_2 = 0.1$ regarding segment losses of $p_{SL} = p$

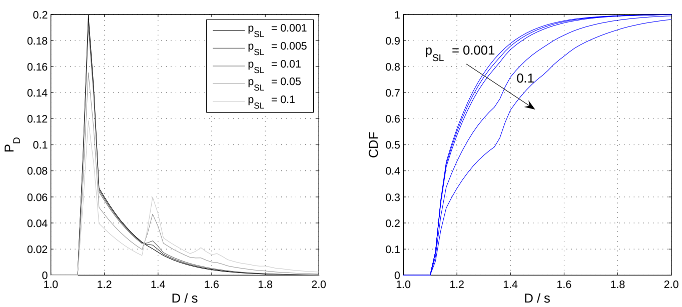

Fig. 11. SR-UDP delay of transmitting 5 kbyte, GPRS downlink, CS-2, MM $p_{22} = 0.8, p_2 = 0.1$ regarding segment losses of $p_{SL} = p$

[7] D.-L. Lu and J.-F. Chang, "Analysis of arq protocols via signal flow graphs," *IEEE Transactions on Communications*, vol. 37, no. 3pp, pp. 245–251, Mar 1989.

[8] M. Rossi, L. Badia, and M. Zorzi, "On the delay statistics of SR ARQ over Markov channels with finite round-trip delay," *IEEE Transactions on Wireless Communications*, vol. 4, no. 4pp, pp. 1858–1868, Jul 2005.

[9] S. J. Mason, "Feedback theory — some properties of signal flow graphs." *Proceedings of the Institute of Radio Engineers*, vol. 41, no. 9, pp. 1144–1156, Sept. 1953.

[10] G. Gehlen, F. Aijaz, and B. Walke, "An enhanced udp soap-binding for a mobile web service based middleware," in *Proceedings of IST Mobile Summit 06*. Myconos, Greece: ComNets, Faculty 6, RWTH Aachen University, Germany, Jun 2006, p. 8. [Online]. Available: http://www.comnets.rwth-aachen.de

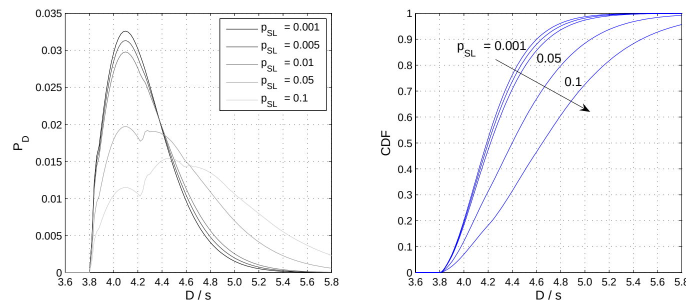

Fig. 12. SR-UDP delay of transmitting 10 kbyte, GPRS uplink, CS-2, MM $p_{22} = 0.8, p_2 = 0.1$ regarding segment losses of $p_{SL} = p$

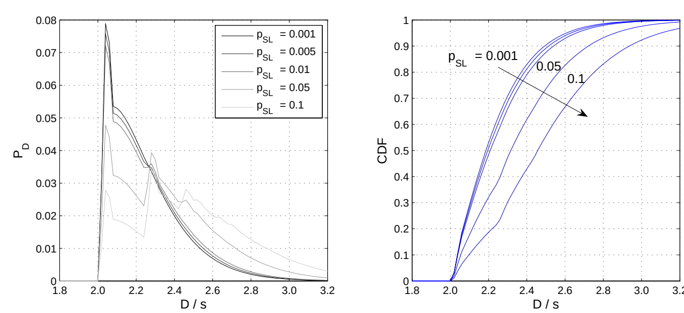

Fig. 13. SR-UDP delay of transmitting 10 kbyte, GPRS downlink, CS-2, MM $p_{22} = 0.8, p_2 = 0.1$ regarding segment losses of $p_{SL} = p$